Materials and Structures (2015) 48:815–833
DOI 10.1617/s11527-014-0486-1

ORIGINAL ARTICLE

Statistical justification of model B4 for multi-decade concrete creep using laboratory and bridge databases and comparisons to other models

Roman Wendner · Mija H. Hubler · Zdeněk P. Bažant

Received: 5 June 2014 / Accepted: 2 December 2014 / Published online: 15 January 2015

Abstract This paper presents: (1) statistical justification and calibration of model B4 using laboratory creep data and long-term bridge deflection data, and (2) statistical comparisons of various types with the existing creep prediction models of engineering societies. The comparisons include the 1995 RILEM Recommendation (Model B3), *fib* Model Code 1999, Model Code 2010, ACI Committee-209 Model, and the 2000 Canadian Model by Gardner and Lockman. The statistics and comparisons rely on a separately presented combined database of laboratory tests and multi-decade bridge deflection measurements, which has been developed at Northwestern University (NU). The laboratory data assembled in the NU database more than double the size of the previous RILEM database. The collected bridge data include multi-decade deflections of 69 large-span prestressed bridge spans, most of them excessive. The multi-decade bridge data are the only available and a significant source for long-term calibration because only 5 % of laboratory creep tests in the database had durations >6 years, and only 3 % are >12 years. Joint optimization of the laboratory and bridge data is conducted. Improved equations are obtained to predict the basic parameters of the compliance function for creep from the environmental conditions and concrete composition parameters, including the water-cement and aggregate-cement ratios, cement content and type, and admixture content. Comparisons with measured individual compliance curves are included as an essential check to validate the form of the compliance function.

Keywords Creep · Database · Calibration · Concrete · Long-term bridge deflections · Statistical evaluation

R. Wendner · M. H. Hubler
Civil and Evironmental Engineering, Northwestern University, Evanston, IL, USA

Present Address:
R. Wendner
Christian–Doppler Laboratory on Life−Cycle Robustness of Fastening Technology, Institute of Structural Engineering, University of Natural Resources and Life Sciences, Vienna, Austria

Present Address:
M. H. Hubler
Civil and Environmental Engineering, Massachusettes Institute of Technology, Cambridge, MA, USA

Z. P. Bažant (✉)
Civil and Mechanical Engineering and Materials Science, Northwestern University, Evanston, IL, USA
e-mail: z-bazant@northwestern.edu

1 Nature of problem

Within the service stress range of structures, the constitutive law for concrete creep may be assumed to be linear in stress, i.e., to follow the principle of superposition in time. The creep Poisson's ratio is

approximately constant and the material can be treated as isotropic. These facts make it possible to characterize the creep of concrete in terms of a uniaxial compliance function, whose generalization to a three-dimensional constitutive law is straightforward. But there are some complications.

One is the aging of concrete, which is caused by cement hydration during the first year (or first few years), and by microprestress relaxation for multi-year and multi-decade creep. Another is the effect of drying and heating, and generally the environmental conditions, which are accompanied by cracking damage and greatly modify creep. The fact that there are numerous concretes with different compositions and that the designer needs to predict the composition effect on creep is a further complication. So is the need to predict the effects of humidity and temperature. A major complication is that the current design practice needs the creep to be characterized by its cross section average, even though the cross sections of beams or plates exposed to the environment are in a nonuniform stress state, with an evolving pore humidity distribution and growth of microcracking. In view of all these complications, it is not surprising that the progress in mathematical modeling of creep has occupied several generations of engineering researchers and is still incomplete.

It should be emphasized, however, that the future doubtless is a local (or point-wise) material constitutive law for concrete considered as a homogenized continuum. In that case, the creep evolution is different at different points of the cross section, residual stresses and cracking develop, and the environmental conditions become the boundary conditions of a moisture diffusion problem. The local constitutive law is much simpler than that for average cross section behavior but its development and use runs into two problems:

(1) Inverse three-dimensional finite element analysis of stresses, moisture and heat transport, and cracking of the test specimens is necessary to extract the creep law; and
(2) the designer must analyze the structure as a three-dimensional finite element system and the diffusion of moisture as well as heat conduction must be included in the analysis.

The first problem has already been coped with deterministically, for limited data, but at present is hardly tractable for statistical optimization of fits of data from the tests of thousands of specimens. The second problem is forbidding for the current state of design practice. Therefore, one must accept creep characterization in terms of the average creep of a cross section of long members. Only in the case of sealed specimens that are in a homogeneous state with constant moisture content does such a characterization represent a locally applicable point-wise constitutive law.

Here the goal is to calibrate a new prediction model B4 for the average cross-section compliance function. The development of model B4 has been the subject of three preceding papers [1–3] presenting the model equations, the optimization method and the statistics of the shrinkage formulation. Model B4 is a generalization and improvement of model B3, which became a RILEM Recommendation in 1995 [4–6], and of the slightly updated version in [7].

The functions defining the relations of the basic parameters of the compliance function to the composition and strength of concrete and to the environmental conditions are here identified and optimized. This is done with the help of a new large laboratory database featuring about 1400 creep tests, and another database featuring multi-decade deflections of 69 bridge spans, both assembled at Northwestern University [1, 8]. Model B4 is then statistically compared to the preceding RILEM Model B3 and to four other prediction models of engineering societies.

1.1 Overview and explanations of B4 and compliance functions to be compared

The compliance function in model B4 has the same form as in model B3 [4, 9], with two exceptions. One is that minor improvements are made in the equivalent times introducing the temperature effect. The second is that, unlike B3, the drying creep part of the B4 compliance is related only to the drying part of shrinkage, rather then to the total shrinkage, since in model B4 the drying and autogenous parts of shrinkage are split into separate functions. This is a refinement that is important primarily for high strength concretes for which, in contrast to normal concretes, the autogenous shrinkage is not a negligible part of total shrinkage.

The B4 compliance function represents a smooth transition from the double-power law for short creep durations $(t - t')$ [10–13] to a logarithmic law for long

multi-decade durations [14–16]. The compliance function is a linear combination of the instantaneous compliance, three terms for the basic creep (i.e., creep at constant humidity and temperature, as in sealed specimens) and one more term for the drying creep (also called the Pickett effect). The three terms for basic creep consist of the aging and non-aging creep terms, and the long-time age-dependent viscous flow.

An important advantage of the B4 and B3 models is that the compliance function satisfies the non-divergence condition. This ensures that the creep recovery curves obtained by superposition are always monotonic, with no recovery reversal which is unrealistic and thermodynamically objectionable [17]. Other models (e.g., ACI209, MC99, MC10, GL) violate the non-divergence condition, which is a fundamental shortcoming, amply discussed before. Another condition is that the relaxation curves calculated by the principle of superposition must never cross into the opposite stress sign, which is again satisfied by models B3 and B4, see Figs. 1 and 2, but not others.

The aging aspect is based on the microprestress solidification theory [18]. The drying creep term has the size effect and asymptotic properties based on diffusion theory of moisture transport. Despite combining several terms reflecting various creep mechanisms, the B4 (as well as B3) functional form retains smoothness. This form was shown to be able to fit accurately complete test curves of normal concretes over a broad time range, for the longest as well as the shortest load durations in [13], and probably the same applies to high strength concrete (except that there seem to be deviations from this form at very early ages for concretes with high contents of some admixtures, which would probably require introducing an additional term). The basis of model B4, as well as B3, is the solidification theory, which is important from a fundamental theoretical point of view. It is generally impossible to define thermodynamic potentials when the material properties are considered as functions of time. One must choose material properties that can be defined so as to be constant. In the solidification theory, this is achieved by considering that the properties of a constituent, the hydrated cement gel, are constant while the aging on macro-scale results from an increase of the mass fraction (or concentration) of this constituent, as new hydration products are gradually attached to the pore surfaces and thus stiffen the material. After the hydration ceases, the multi-year and multi-decade aging is, in the microprestress theory, fundamentally explained by relaxation of the tensile microprestress, which balances the disjoining pressures in nanopores and facilitates the shear ruptures of interatomic bonds responsible for creep. The formulation based on these two mechanisms of aging violates no tenets of thermodynamics.

Note that all the creep tests used for calibration were conducted under centric uniaxial compression. Therefore, the available models including B4 can have large errors in the case of bending or highly eccentric loads. The reason is that the microcracking distribution and the interaction of stress distribution with pore humidity are different. However this is not a problem for bridge box girders when the walls are subdivided into through-thickness finite elements because the eccentricity of the compression resultant in each such element is always minor.

Also note the reason for introducing $t_0' = \max(t_0, t')$ into Eq. 35 of [2], along with restricting that equation to $t \geq t_0'$ and redefining $C_d(t, t', t_0) = 0$ if $t < t_0'$. This modification, introduced earlier in the 2000 version of B3 [7, Eq. 1.14], prevents C_d from becoming negative when $t' < t_0$, i.e., when the load is applied before exposure to drying. This case is infrequent in practice but may occur, e.g., in segmental cantilever concreting of box girders if the prestress is applied before striping the form or another sealant. It must be admitted that there are no longer-term creep data for this case, but the use of t_0' is the most logical fix.

The ACI [19–21], MC99 [22], and GL00 [23, 24] compliance functions for creep are not composed of separate additive terms for the basic and drying creep. This split and the logarithmic form of long-time basic creep were co-opted from B3 (and its predecessors) for the latest revision of MC10 [25] in 2012. In all the models, except MC10 as adjusted in 2012, the compliance curve for basic creep reaches a horizontal asymptote. The existence of such an asymptote has been an illusion for a century (stemming from the unfortunate habit to plot the creep curves in a linear scale). In the ACI model, this asymptote is reached very soon, which is why that model badly underestimates multi-decade creep. On the other hand, in the GL model the approach to this fictitious asymptote is postponed beyond the times of practical interest. The violation of the non-divergence condition, the cases of

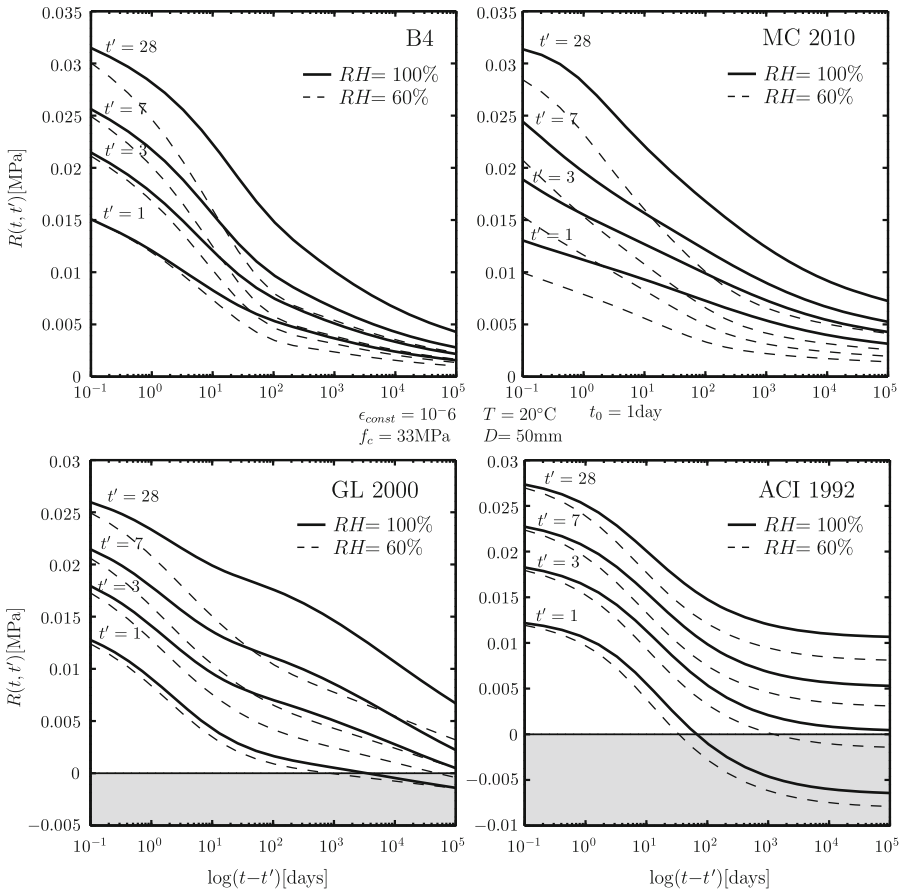

Fig. 1 Relaxation curves calculated by the principle of superposition for sealed conditions (*solid lines*) and relative humidity of 60 % (*dashed lines*)

relaxation ending by a change of sign, and the impossibility to formulate properly the thermodynamics in presence of aging are what plagues all these models.

Additionally, the effect of the specimen size is incorrectly introduced in ACI and MC99 models by vertical scaling of the compliance function rather than by its horizontal shift in the log-scale. None of the established models is able to predict realistically the effects of concrete composition, cement type and, in particular, the effects of admixtures and aggregate type. These effects, which represent a major improvement of model B4 over Model B3, are the focus of this work.

1.2 Engineering practice, creep coefficient and choice of *E*-modulus

It is important to comment on the historical preference of engineers to calculate creep effects in structures using the creep coefficient $\phi(t,t')$, as opposed to the total compliance $J(t,t')$. As long as the approximate age-adjusted modulus method (AAEM, [17, 26–28]) is used there is, of course, nothing wrong in using ϕ, provided that $\phi(t,t')$ is calculated from compliance $J(t,t')$.

The AAEM (recommended by ACI-209 since 1982, by CEB since 1990, and by Model Code 2010) represents a significant improvement over the 1967 Trost method [29] which is still used in commercial bridge creep programs although it is not simpler and is often quite inaccurate due to its shortcomings. The Trost method uses a semi-empirical "relaxation coefficient" unrelated to $J(t,t')$. It does not take into account the ageing of elastic modulus E and expresses the incremental Young's modulus for the time period from t' to t simply by $E'' = E_{28}/[1+\rho\phi(t,t')]$, where ρ is Trost's empirical relaxation coefficient (typically fixed as 0.8) and E_{28} is the constant 28-day modulus. A simple replacement of E_{28} by $E(t)$ and of ρ by the

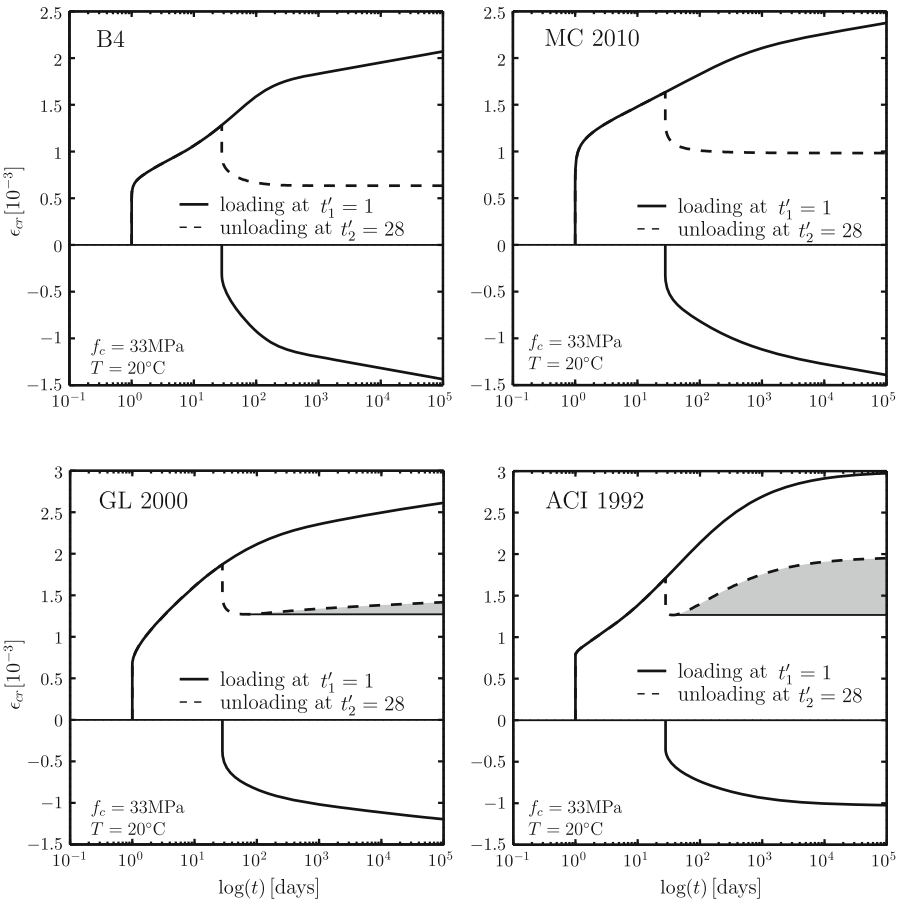

Fig. 2 Creep strain development due to loading at t'_1 =1 day and unloading at t'_2 =28 days

aging coefficient χ, as shown in [27], ensures exact results according to the principle of superposition for a broad range of strain histories and provides simple yet accurate approximations for many practical problems [26, e.g.].

The creep coefficient ϕ by itself is meaningless as a material characteristic, even though engineering societies suggest otherwise. The only thing that matters for creep effects in structures is the total compliance, which may be obtained as $J(t,t') = [1 + \phi(t,t')]/E(t)$. For long-time creep effects in structures the choice of the E value is unimportant provided that the creep coefficient is calculated from $J(t,t')$ as $\phi(t,t') = E\,J(t,t') - 1$. In other words, what is essential is to use the correct combination of ϕ and E.

Based on the compliance, $E(t') = 1/J(t' + \Delta, t')$. In testing practice, the choice of Δ can vary from 0.1 s (as in creep tests started by releasing a compressed gas valve) to $\Delta = 0.1$ day (as in standard creep frames with a manually tightened spring). Because of high (usually ignored) short-time creep, the difference in E can be as big as 25 %. Nevertheless, when both E and ϕ are calculated from J, the long-time structural creep effects obtained using AAEM are about the same regardless of the choice of Δ.

Unfortunately, many experimenters report only the creep coefficient and do not give enough information about the corresponding elastic modulus value. Many data sets report nothing in this regard and thus the compliance cannot be uniquely reconstructed. Because of this, dozens of such data sets had to be omitted from the present analysis.

A further problem arises from the fact that most engineers evaluate E from the code formulas of ACI, CEB and *fib* and then combine it with the recommended ϕ value which is incompatible. The code formulas are intended mainly for determining the deflections under traffic loads and the vibration frequencies (since E is measured after several unload-reload cycles). Big mistakes occur when this

kind of E is combined with ϕ determined from tests as the ratio of creep strain to some unspecified sort of initial deformation.

The subsequent sections will show that the B4 compliance predictions are superior to those obtained by other widely used models, in particular ACI92 and MC99. This statistical proof outweighs any intuitive considerations based on the fact that some of the empirical formulations linking the parameters of the B4 (or B3) creep model to composition information deviate from the trends suggested in other models.

Some may, for example, object that, according to *B*4, the creep coefficient ϕ increases with increasing strength while the *fib* formulation (MC99,MC10) indicates a decrease of ϕ. But there is nothing fundamentally illogical about this B4 feature. Indeed, physical reasoning suggests that lowering the water-cement ratio, w/c, should have more effect on the increase of elastic modulus, due to stiffening of the porous microstructure, than it does on the decrease of creep rate, which is governed by the rate of breakage of C-S-H bonds on the atomic scale. These are physically different phenomena, with different mechanisms. Of course, if the increase of E due to decrease of w/c is considered smaller than the correct value, then one can incorrectly infer an increase of ϕ. For similar reasons, one cannot object to an increase of ϕ with the age age t' at loading.

1.3 Effects of temperature, cement type and admixtures

Model B4 [2] introduces equivalent times based on Arrhenius-type equations for the temperature effects on the creep rate, aging (or hydration) rate, and drying shrinkage rate. In principle, their activation energies can be different but, because of data ambiguity, the activation energy U of each is considered the same ($U/R \approx 4{,}000$ °K, R = gas constant), as formulated in [13] and roughly supported by several experimental studies [30, 31]. This temperature dependence does not apply above 75 °C, because of phase changes and because different activation energies dominate in different temperature ranges.

In basic creep, the activation energies of creep rate and of hydration compete with each other, the former accelerating and the latter decelerating the creep as temperature rises. The effect of the latter disappears once hydration is complete (i.e., after about 1 year). The drying part of creep also depends on the activation energy of drying (or diffusion process), which leads to an acceleration of the drying creep term when the temperature is raised. These effects are captured in model B4 by a series of scaling parameters.

Admixtures have a smaller effect on creep than on shrinkage. The effects of water-reducers, retarders, superplasticizers, air-entraining agents, accelerators, shrinkage reducing agents and mineral admixtures have been studied for creep. Many test data on the effects of cement type and of admixture type and amount exist, but they are so scattered that no systematic trends can be detected.

The differences in the effects on the rate and the magnitude of total creep attributable to admixtures depend on their diverse effects on evolution of microstructure. There is no consensus on the contribution of water-reducers and superplasticizers, as the data lie in the range of experimental uncertainty. While some tests in the database indicate that the addition of accelerators and the fly ash replacement exceeding 15 % systematically cause some increase of creep, generally the air-entraining agents, shrinkage reducing admixtures, and low amounts of fly ash replacement are found to have no consistent, systematic and statistically verifiable effect on creep.

The high strength concrete has been shown by various researchers [32–34] to have a creep coefficient about 1.8–2.4 times smaller, However, the creep effects on the structural scale are often greater because the cross sections are often much thinner and the elastic modulus is about 2–4 times larger. The creep reduction is due to the lower w/c ratio and the addition of silica fume or fly ash. The self-consolidating concrete has similar creep as the normal concrete [35].

What is clear at present is that the effects of these six admixtures are highly variable statistically and no unique time functions exist. For the mean behavior it seems sufficient to introduce empirical coefficients that scale only the creep magnitude. As for the effect on multi-decade creep in particular, no data exist. Recalibrations should be performed in the future as new data become available.

Similar studies were made for the effect of cement type on the basic and drying creep. Calibrated parameters capturing the cement type dependence exist in all models for creep. The European classification of R—normal, RS—rapid hardening and SL—

slow hardening is selected for model B4 since it is directly related to the reaction rate of the cement instead of the type of application, which is the basis of other classification systems.

Predictions are complicated by the fact that cement classifications as well as cement products and production standards have changed over time and various cement replacements have been introduced. This engenders a large scatter and uncertainty in the model calibration. The type of cement used shows a strong correlation to the observed basic and drying creep when using the data in the NU database. On the other hand, contrary to shrinkage, there is little correlation to the aggregate type classes. Even though an effect of the aggregate type is perceived to exist [36] there is a lack of consistent and repeated test data. For each type of aggregate there exist only a limited few curves, in the current NU database at most 6, which is not enough for statistical inferences.

1.4 Optimization of fit of combined laboratory and bridge databases

Large bridges and other creep sensitive structures are generally designed for service lives of 50–150 years. However, 95 % of the laboratory creep tests available in the largest worldwide laboratory database [1] with 1370 creep curves do not exceed 6 years in duration. Only 3 % of the data sets, many of them with questionable reliability of long-term measurements, exceed 12 years.

Consequently, the laboratory data used for calibration of a creep model must be supplemented by inverse inference from multi-decade structural observations. Most informative for that purpose are the data on deflections of large-span prestressed concrete segmental box girder bridges, provided that the deflections are excessive (if they are not, it means that a large gravity deflection is offset by a large upward deflection due to prestress, which is a small difference of two large random numbers and is too scattered to be useful). Data on multi-decade shortening of prestressed bridge girders would be useful even if the deflections are small, but such data are unavailable. Data on multi-decade shortening of columns of tall buildings would also be useful but are unavailable as well.

The most useful bridge paradigm is the K-B bridge in Palau [37], built in 1977. Within 18 years it deflected by 1.61 m compared to the design camber. Probably it would not have received special attention if remedial prestressing in 1976 did not cause it to collapse (after a three-month delay, with falalities). The data, sealed in perpetuity after court litigation, were fortunately released in 2008 (as a result of a resolution of Structural Engineers World Congress). It was found [37] that the creep equations in the standard recommendations or design codes of engineering societies severely underestimated the mid-span deflections. Their predictions amounted to 31–43 % of the measured values, and 57 % for the theoretically based Model B3, which is a 1995 RILEM recommendation.

The new Northwestern University (NU) [1] database, which more than doubles the size of the previous laboratory database [38], includes also the data on relative multi-decade deflection histories of 69 large bridge spans from nine countries and four continents [8]. These data are used in statistical inverse analysis, and are crucial for calibrating the terminal trend of creep. A complete inverse analysis was unfortunately impossible due to a lack of information on the concrete composition and strength, structural geometry and prestressing for most of the bridges.

Instead, based on the method formulated in [8], the mean terminal deflection development was transformed into an approximate terminal compliance evolution based on estimating likely average properties of these bridges and their concretes. These estimated properties included: the required design strength, which was converted to the mean strength of concrete, the average effective cross-section thickness, the environmental humidity (based on the bridge location), and the cement composition. Errors stemming from these simplifying assumptions mostly compensate each other in a statistical sense, and so the mean relative compliance development deduced from all the 69 bridge spans is probably roughly correct even though the absolute residuals $J - \hat{J}$ are, of course, rendered meaningless by these estimations.

The analysis of bridge data showed a systematic underestimation of the terminal trend of creep and led to an adjustment of the compliance function that minimizes the error in matching the terminal deflections of these 69 bridges. In the optimization, the

transformed bridge deflection data were considered to have 1/3 of the total weight (and the laboratory database 2/3). The terminal bridge deflections were introduced only for optimizing the parameters that control the terminal slope of the compliance function in the logarithmic time scale. Since the database mostly contains data of much shorter durations (<6 years), only the scaling parameters (and not the formulas for the intrinsic and extrinsic influences) were optimized for the bridges. Thus the optimization of the effects of concrete composition and environment was not biased by the incompleteness of bridge data.

1.5 Parameter identification and optimization method

While the initial goal of the update of the creep model was solely a recalibration (keeping the functional form and theoretical foundation of Model B3), five assumptions in the model were re-examined before proceeding with the optimization process.

The first is the initial elastic modulus for static load application. As mentioned in Model B3 RILEM recommendation 107-GCS [4], the inverse of the 28-day elastic modulus given by the ACI empirical equation corresponds to the compliance for 5–20 min after load application. However, a better agreement can be reached between the standard 28-day modulus and total compliance after roughly 1–2 min ($\Delta = 0.001$ days). This conclusion is the basis of the calibration of Model B4 as well as B4s. Figure 3 shows the comparison of the B4 and B4s compliance predictions with E_{28}.

The approximate age independence of $q_1 = 1/E_0$ (previously shown in Fig. 6 of [5]) has been verified and is illustrated in Fig. 4.

Second, the exponents n and m of the load duration and age [2] were calibrated by short to medium range data from the NU database as well as nano-indentation creep data for cement paste obtained by Vandamme et al. [39]. Only the basic creep tests of normal concrete, unaffected by drying and autogenous shrinkage, were used in this analysis. Unbiased optimizations with different starting points confirmed that, in an average sense, the previously assumed parameters $n = 0.1$ and $m = 0.5$ [5] still provide the best and,

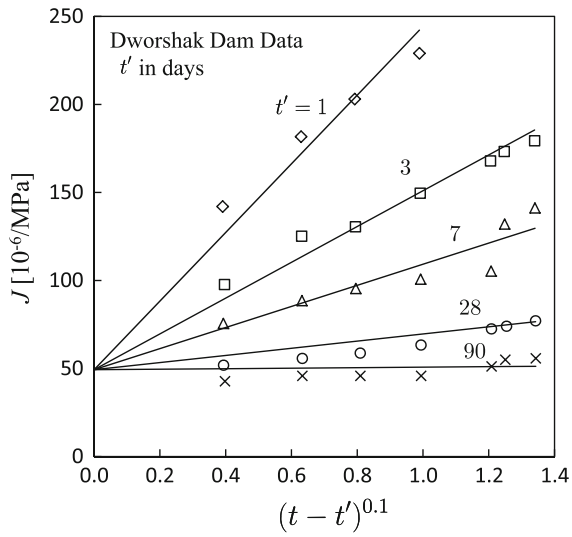

Fig. 4 Fit of the Dworshak Dam data demonstrating that the short-time creep data confirms the age-independence of $q_1 = 1/E_0$

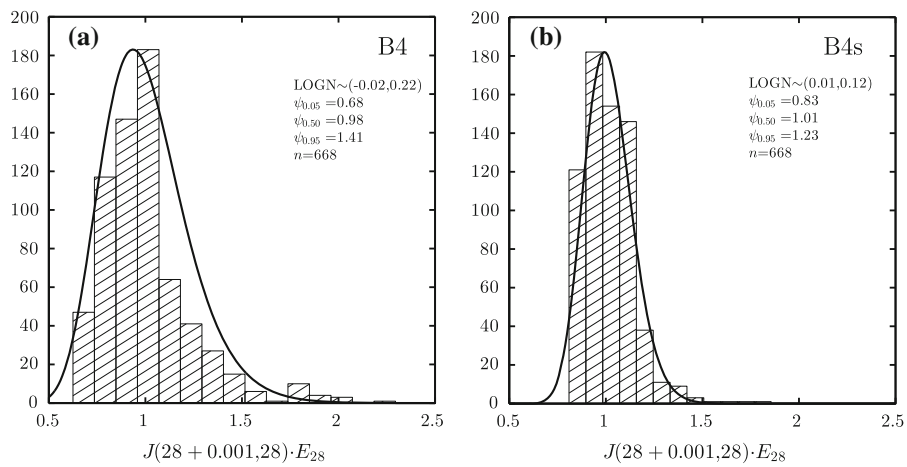

Fig. 3 Agreement between E_{28} and creep compliance after $\Delta = 0.001$ days for **a** Model B4, and **b** Model B4s

more importantly, consistently good, fits. For certain compositions, the prediction quality could be improved by varying n between 0.08 and 0.12. However, no consistent trend or dependency on composition parameters or cement type could be identified.

Third, the calibration of the creep model was in general highly sensitive to the value of the initial elastic strain. So, exponent p_1 in the estimation of the instantaneous compliance in terms of the 28-day Young's modulus [2] had to be optimized first and then prescribed for all the subsequent optimization steps. Two approaches were pursued and turned out to yield similar results: optimization of the full formulation of model B4 (with fixed average long-term parameters) and a linear fit in power-law scale of the short-term test data with at least 3 measured data points within the first minutes to hours of measurement, depending on the age of concrete at load application (e.g., up to 4 hours for concretes loaded at 7 days). The limit is based on an empirical formulation that is derived for the functional form of model B4 based on sensitivity studies.

Fourth, as in Model B3, the basic creep formula for the aging viscoelastic compliance rate is given in a closed form, which is all that is needed for step-by-step computer analysis of structures. But its integration leads to a binomial integral $Q(t,t')$ that cannot be evaluated in closed form. Although its numerical evaluation is easy, an approximate formula for function $Q(t,t')$ is available [2, 4, 7]. It applies equally to model B4 and it has been checked that it has a four digit accuracy within the range of interest.

Fifth, recent important test data from M.I.T. on nano-indentation creep [39] have also been analyzed, for validation purposes. Since the tests were made on hardened cement paste, the compliance magnitude cannot be compared with the tests on concrete, but the exponent n of the load duration must be about the same. Figure 5 shows the measurement data for durations $t-t'$ from 0.1 to 200 s, compared to the best fits by a logarithmic time function, by a power law with exponent $n=0.1$, and a power law with optimum exponent. Sampling bias towards later ages with denser point spacing was removed through a weighting scheme with equal weights for each half-decade in the log-scale.

The overall fit in Fig. 5 clearly shows that an exponent $n=0.10$ is a good approximation. The best fit, with $R^2>0.99$, is attained for $n=0.089$ (R = coefficient of determination). The logarithmic time-function (which corresponds to $n\to 0$) is a fair approximation but by no means an optimum. Figure 5b shows the fit to the first measurements for durations <1 s and its extrapolations to longer times. Again $n=0.10$ works well [the optimum fit within (0.1, 1 s) leads to exponent $n=0.577$, but the reason is that inserting the indenter took much longer than 0.1s].

The next stage required re-evaluating the form of the dependence of material parameters on concrete composition. The existing model (B3) depended on both the mix characteristics (i.e., the water-cement ratio, aggregate-cement ratio, and cement content) and the mean mechanical characteristics (i.e, the 28-day strength and the Young's modulus). It is well known that water-cement ratio, compressive strength and

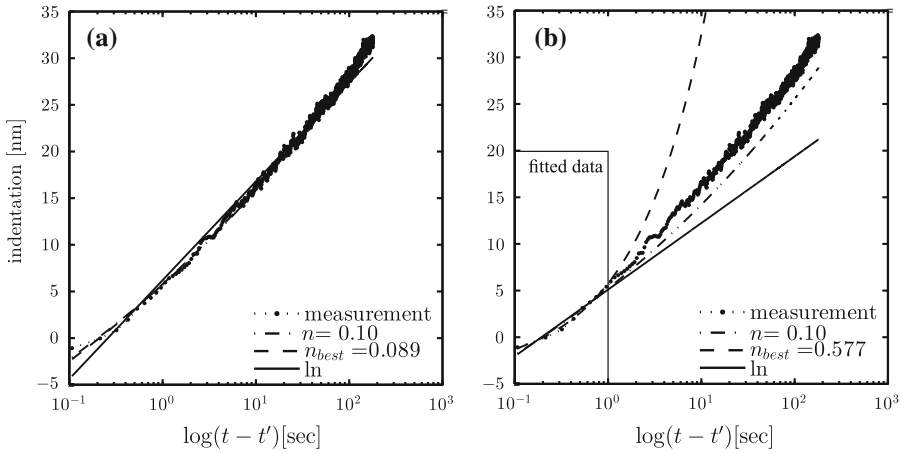

Fig. 5 Best fit of nano-indentation test data by Vandamme et al. [39] by logarithmic time function, power law with exponent $n=0.1$, and power law with optimum exponent: **a** fit of the full data range, **b** fit of first second only

Young's modulus are highly correlated. With decreasing w/c, both the strength and the elastic modulus increase. As a consequence of this high correlation, a simultaneous use of the strength and w/c brings about little gain and in fact makes the optimization problem ill-conditioned, yielding arbitrary and non-unique results. Furthermore, the compressive strength typically only serves as a convenient indicator for other material properties.

Therefore, two sets of predictor equations, for two versions of model B4, have been formulated and calibrated, one using the mix proportions only (named B4), and one using the mean compressive strength only (named B4s). Young's modulus is used in both versions since it is the most important characteristic for the instantaneous deformation.

All the effects of composition and strength enter the material parameters in the form of products of power functions. This has the advantage of a linear relation between the logarithms of the input and response and thus helps convergence of the optimization (another reason for power functions is that they are self-similar, which is appropriate when no characteristic value is known). To keep the input values dimensionless, these functions have all been normalized by their respective mean values. This avoids most dimensional inputs, which also minimizes the chance of user's error in dimensions.

The water-cement ratio was found to be the most important input parameter for the magnitude of all the components of the compliance function. This is consistent with other studies and agrees with the creep mechanisms considered in the micro-prestress solidification theory [18]. The second most important is the aggregate-cement ratio, which affects the non-aging viscoelastic creep, the flow, and the drying creep terms of the compliance function.

The individual influencing parameters were identified by a step-by-step procedure using various statistical approaches. At first, the potential influencing parameters were selected as those reported by most experimenters. The objective was to identify the relations of these parameters to the basic parameters $q_1, \ldots q_5$ (see [2]) of the B4 compliance function, as well as to the scaling factors for temperature, various admixtures and the cement type. For each unknown relation, for example, the effect of water-cement ratio on the scaling factor of the non-aging viscoelastic creep term, one could identify on the creep curve the time range of maximum sensitivity (one or a few decades in the logarithmic time scale).

Subsequently, the relations of model parameters [2] to input material parameters affecting this time range were optimized, so as to minimize the C.o.V. of the differences between the predicted curve and the data points in this time range (relative to the mean of data, not of the differences) [3]. The optimization also yielded an R^2 error measure, a full Jacobian matrix for sensitivity analysis, and the fit of each curve for visual shape analysis. The evaluation of the Jacobian matrix revealed correlations between the model parameters and the input properties, as well as between both groups. This process allowed adjusting the formulation and a converged selection of input material parameters of the creep model (for normal concrete under standard conditions). Further scaling parameters were introduced to capture the effects of temperature, admixtures and cement type. The general optimization algorithm, strategy, and process used to develop the full model B4 are described in a preceding paper [3]. The exponents p_1 and p_2 of the scaling factors in basic creep, and p_5 in drying creep [2], showed the strongest dependence on the cement type. The effects of admixtures were best described by modifying the exponents p_2, p_3, and p_4 for basic creep and p_5 for drying creep [2].

The changes in functional form of the B4 creep formula are sketched in Fig. 6. For standard conditions, an increase in w/c increases the creep rate as well as the vertical scaling factor of the creep curve. A decrease in the relative humidity of the environment increases the vertical scaling factor but has no significant effect on the halftime of the creep function, which gives the horizontal scaling in a linear time plot (or a horizontal shift in log-time plot). An increase of temperature generally engenders in the database concretes an increased rate and magnitude of creep (except possibly for very young concretes for which the hydration acceleration, which reduces creep, may prevail). The last diagram in the figure shows the change in the creep curve shape due to a change of cement type.

1.6 Verification of the shape of predicted individual curves

As described in the previous paper of this series for shrinkage [40], a separate statistical analysis aimed at

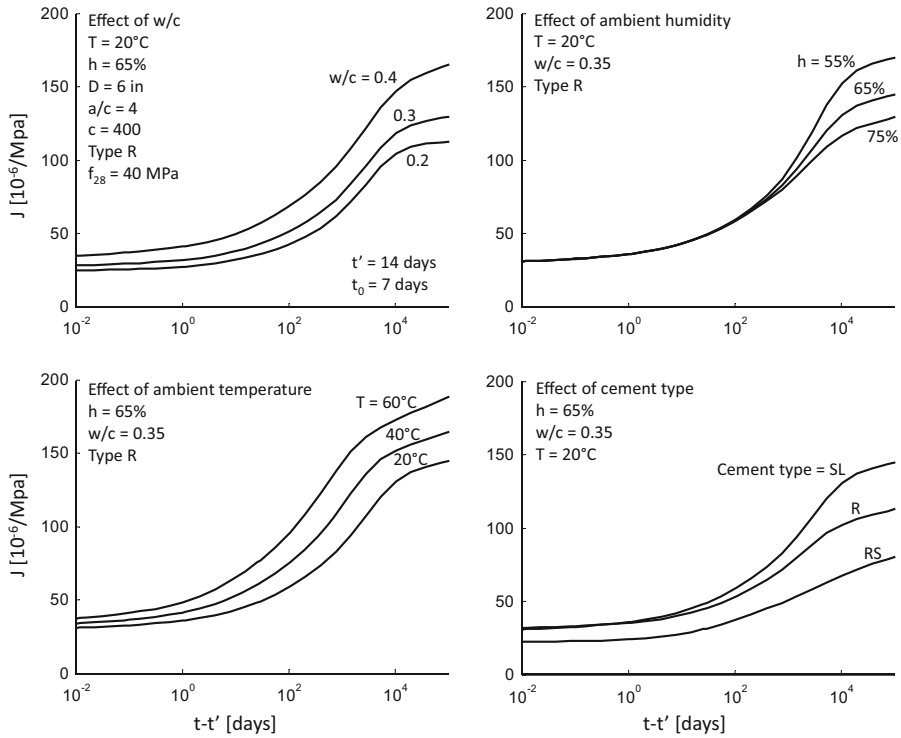

Fig. 6 Trends of variables associated with the B4 creep curve

verifying the shape of model B4 creep and shrinkage curves was performed at the outset. If the shape of the individual curves of some model is not realistic, it makes no sense to optimize that model by the database. However, by comparisons to the entire database it is impossible to check whether or not the shape of the creep or shrinkage curves is correct because the database scatter due to concrete type, composition and admixtures dwarfs and obscures any strange features in the curve shape.

Figure 7 shows such comparisons of the model B4 curves with individual measured curves, using only the data from the tests whose duration range was long enough for the comparison to be meaningful. Figure 8 shows similar individual comparisons for the curves of the ACI92 model. To examine the capability of the general form of the models, the composition dependent horizontal and vertical scaling parameters have been optimized, consistently for all the curves of each concrete batch.

These graphical comparisons are followed by statistical comparisons in terms of bar charts documenting the capability of the form of each model to capture the shape of the individual creep curves (Fig. 9) as a function of load duration $t - t'$ and their dependence on the age t' at loading. Bar charts are also used to compare the optimum fits of the full database (Fig. 10). A detailed study of the development of residuals gives insight into the model calibration. Furthermore, an uncertainty quantification of the main parameters of model B4 is presented.

Example fits in the top row of Fig. 7 show the capability of model B4 to fit tests of long durations or a broad range of ages at loading, selected from the NU database. The bottom row shows that test series with broad variations of environmental conditions (temperature and humidity) and specimen size can also be fitted well. The trends in the experiments on the same concrete could be recreated with a C.o.V. of less than 10 % even though only the free scaling parameters were adapted, consistently, of course, for all curves of the same series (and thus the same concrete). None of the parameters influencing the dependence on t', T, V/S, h were changed. Depending on the particular form of each model, the number of free parameters varied between two (i.e, the initial deformation plus the multiplier of the creep part of compliance) for ACI and other models, and five for model B4. The dependence on the investigated parameter was not changed in any case.

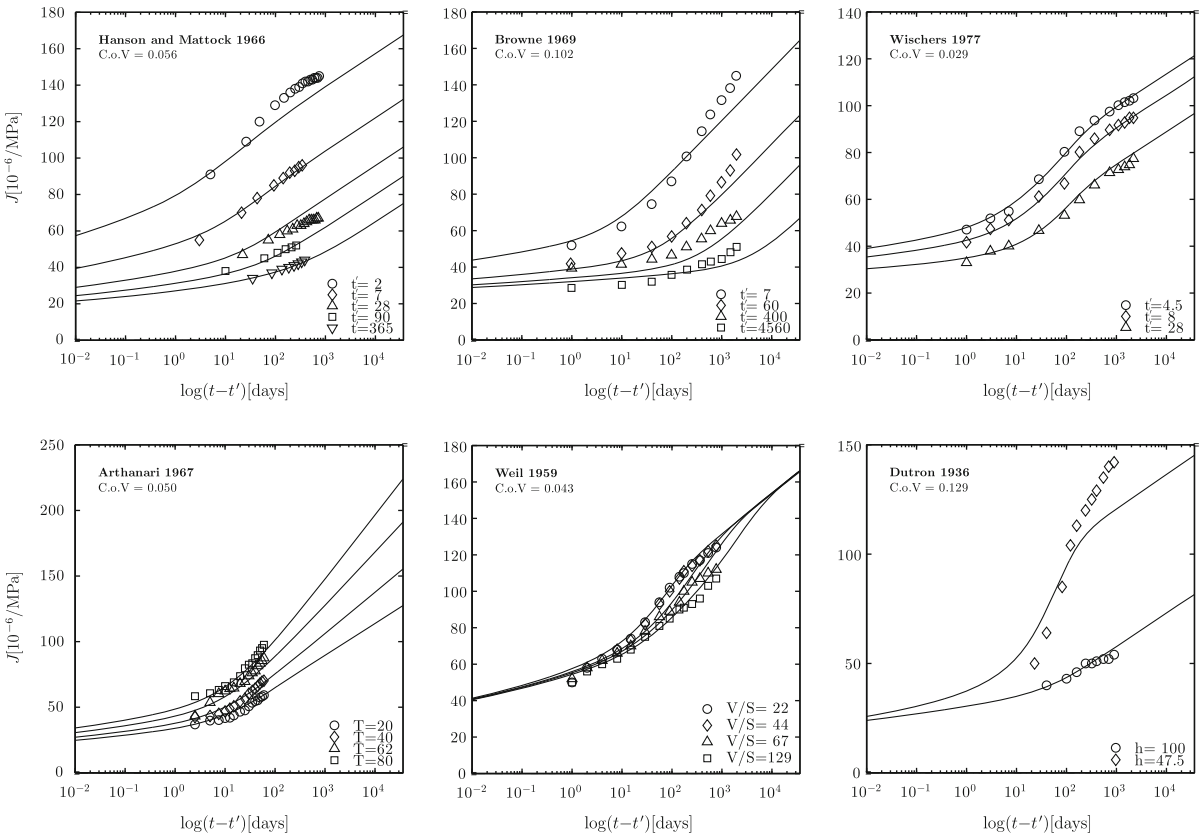

Fig. 7 B4 example fits of select creep test curves

Table 1 defines the creep time function, the number of intrinsic parameters (as a gauge of function flexibility), and the number of fitted parameters used for each model. Intrinsic parameters are herein defined as those parameters that describe the concrete composition, such as $w/c, a/c, c$, but also the strength and elastic modulus. In addition to a visual evaluation of the capability of the model to capture the shape of the creep curves, shape statistics are also calculated using a selection of curves with sufficient data in the initial and final range. The resulting comparisons based on the laboratory data are presented in Fig. 9. A number of inferences can be made from this comparison.

If only the data sets with the influence of drying are analyzed, see Fig. 9 (top left), model B4 based on concrete composition outperforms the other models, followed by B4s. The reason is that it can separate the drying shrinkage from the autogenous shrinkage and thus realistically describes the influence of drying creep in the presence of admixtures. Models without this split in autogenous and drying shrinkage (GL00 and ACI92) perform worst for total creep, even though the quality of fit for basic creep (no influence of drying) is only slightly inferior. It is interesting to note that the now replaced MC99 outperforms all other models except B4 and B4s with regard to short-term basic creep. The combined set of comparisons is presented in the lower row and follows the ranking governed by the influence of drying creep.

After evaluating for various models the functional form of compliance, i.e., the shape of the time curve, the next step is to investigate and compare their capability to predict the dependence on the age at loading. This step is omitted here for the sake of brevity as the findings are already detailed in the preceding paper [3].

The third step is to investigate and compare the overall prediction quality, considering the full NU database. To distinguish the quality of fit in early and later stages of creep, we first separately consider the laboratory data (mostly <6 year in duration) and the

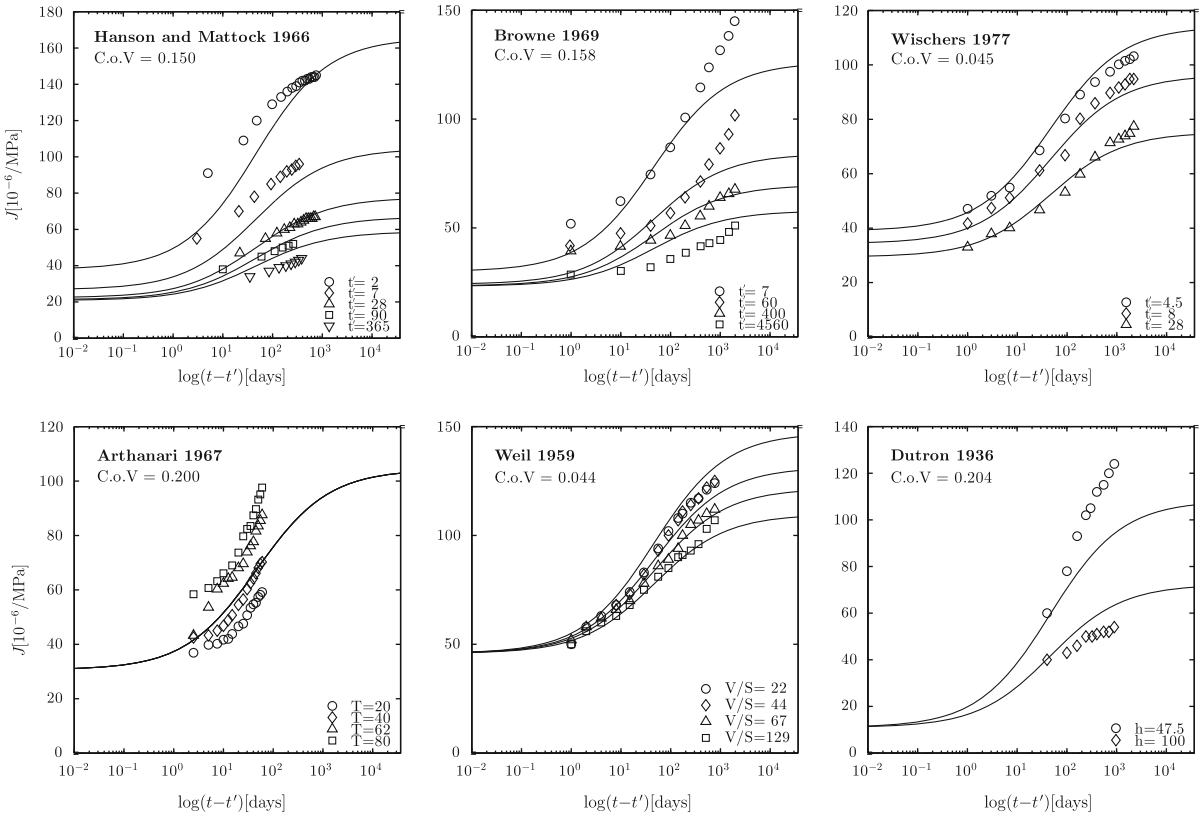

Fig. 8 ACI92 example fits of select creep test curves

multi-decade bridge data. Figure 10a, b show the quality of fit of different models for the laboratory data only, and Fig. 10c shows the same for the multi-decade relative bridge deflections. The combination of long-term laboratory data (longer than 1,000 days) and relative bridge deflections is given in Fig. 10d.

The C.o.V. of residuals for short-term laboratory creep test data is found to be the lowest for the B4 and GL models. Their near equivalence may be due to the similar flexibility of the time function used and the fact that the GL model was empirically based on a carefully handpicked selection of creep tests that showed a clear trend in time rather than the complete data set, as has been done with the B3 and B4 models. In terms of global statistics MC10 outperforms its predecessor MC99 for short-term creep and reaches a close tie for long-term lab data even though the individual shape statistics of Fig. 9 show the opposite trend. The reason likely lies in a better overall calibration of the model (note that Fig. 9 illustrates the potential of the formulation, not its calibration). Model B3 suffers from the missing split in autogenous and drying shrinkage. This compromises the long-term prediction, due to the distortion of the drying creep component, in spite of its correct functional form as revealed in Fig. 10c. A wrong functional form (horizontal asymptote) as formulated for MC99, and ACI92 is clearly revealed in the statistics of multi-decade structural evidence as plotted in Fig. 10c. The GL00 model is an exception as its functional form corresponds to MC99 but is calibrated in such a way that it approaches a horizontal asymptote only far beyond the longest measurement times and thus mimics a terminal slope of the creep compliance in logarithmic time.

This fact underscores the need for a separate investigation of the functional form, and in particular its asymptotics, see Fig. 10c. Clearly all the models that can capture the correct asymptotics (B3, B4, MC10) or that approach it (GL00) outperform models that do not (ACI92, MC99).

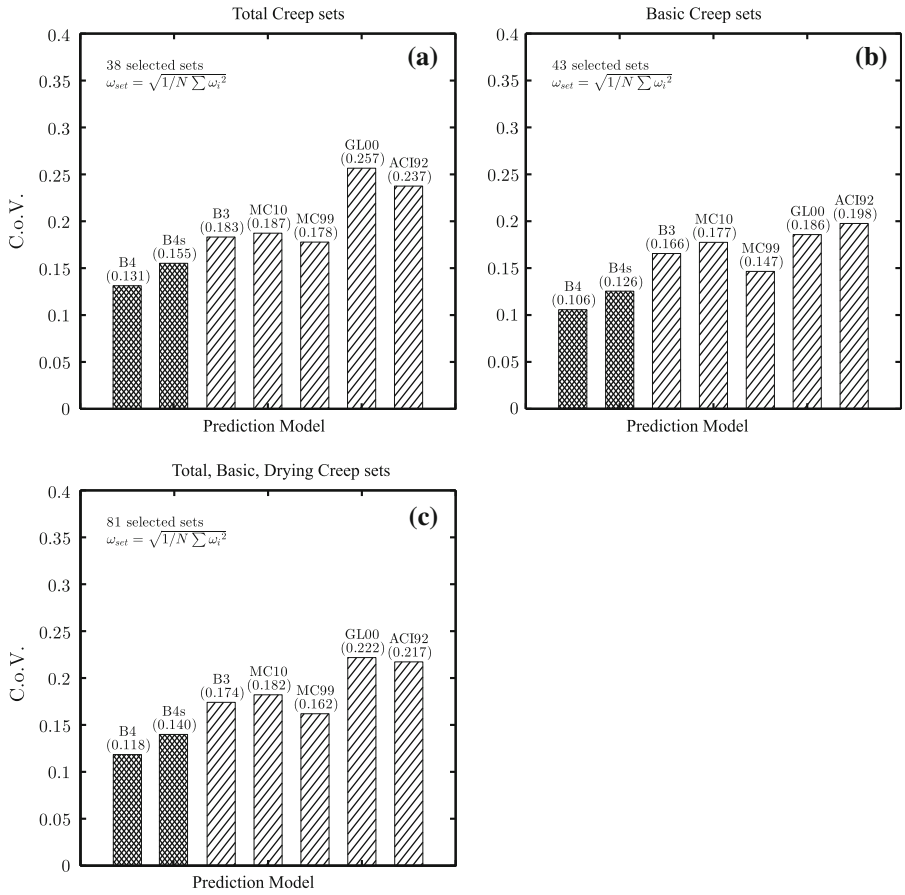

Fig. 9 Quality of fit for subsets of **a** total creep, **b** basic creep only, and **c** combined set, based on absolute values

If the long-term laboratory creep test data are combined with the bridge deflection information, a more balanced perspective of the long-term prediction quality is obtained. As expected, models B4 and B4s show the lowest C.o.V., followed by B3, MC10, GL00. The MC99 model cannot catch up with the competitors but still exceeds the prediction quality of ACI92 by far.

In future studies, in which not only the relative but also actual deflections of bridges should be used for calibration, it will be important to use a realistic model for steel relaxation as affected by temperature and strain variation; see [41].

To give a more detailed insight into the development of the prediction quality, Fig. 11 shows the residuals, $J - \hat{J}$, of all models plotted against $\log(t - t')$. Model B4, and also the simplified strength-based model B4s, consistently show a very small mean value deviation. The scatter band given by the 5 and 95 % percentiles is largely symmetric, which confirms no bias towards over- or under-estimation. The ACI92 and GL00, on the other hand, tend to underestimate creep for long times, as seen in the mean value trend and especially the scatter band. The scatter of MC10, interestingly, is symmetric. But it exceeds the scatter of all the other models in the range between 10 and 1,000 days while decreasing for long times.

To reduce the scatter for long times, information on the concrete composition must accompany future structural measurements. So must the information on the bridge dimensions, prestress and environment.

1.7 Uncertainty quantification

A quantification of model parameter uncertainty is obtained by individually refitting all the creep curves, with scaling of the mean fit, and then analyzing the

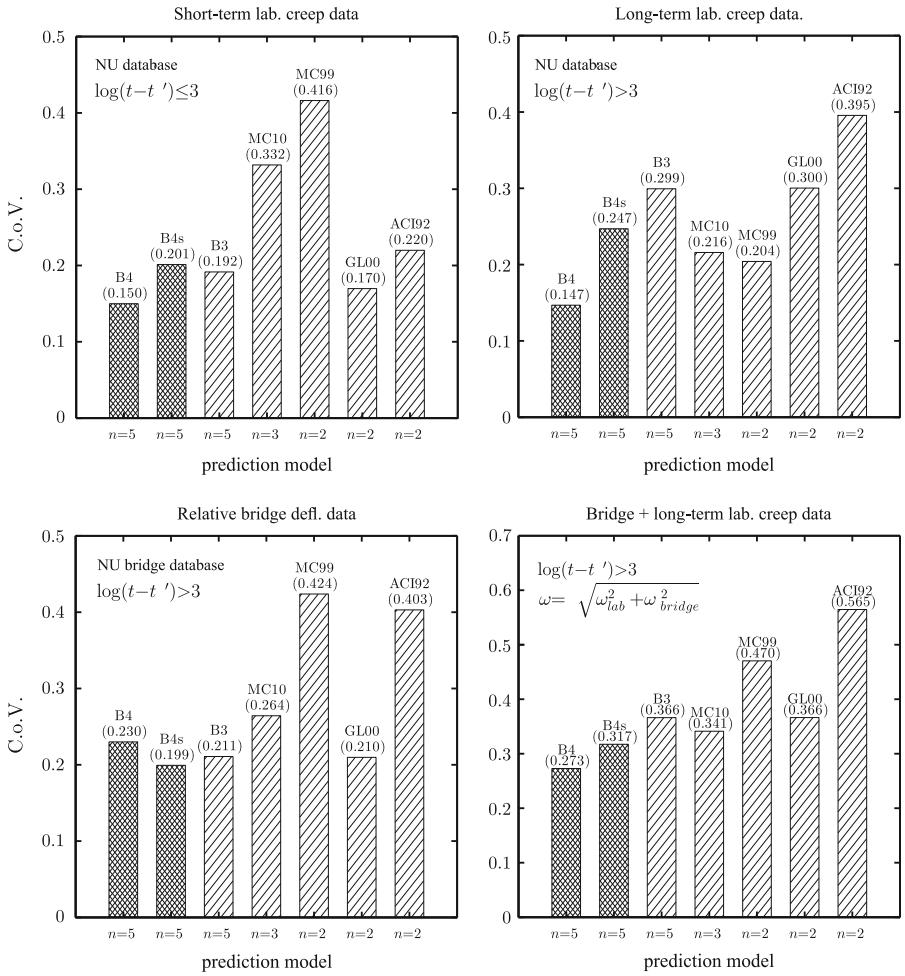

Fig. 10 The quality of fit of the new B4 and B4s models as compared to existing models using the coefficient of variations of residuals as the quantifier

Table 1 Summary of time functions and parameters of various creep models and the corresponding number of intrinsic parameters and fitted parameters used for the model comparisons

Model	Time function	Intrinsic parameters	Fitted parameters
B4	Eqs. 24, 27, 32 [2]	4	5
B4s	Eqs. 24, 27, 32 [2]	3	5
B3	Eqs. 24, 27, 32 [2]	4	5
MC10	$\left(\frac{t}{\beta+t}\right)^{\gamma}$	2	3
MC99	$\left(\frac{t}{\beta+t}\right)^{0.3}$	2	2
GL00	$\beta\left(\frac{t^{0.3}}{14+t^{0.3}}\right)+\gamma\left(\frac{t}{7+t}\right)^{0.5}+\left(\frac{t}{\gamma+t}\right)^{0.5}$	2	2
ACI92	$\frac{1}{\beta}\left(1+\frac{t^{\psi}}{d+t^{\psi}}\right)$	2	2

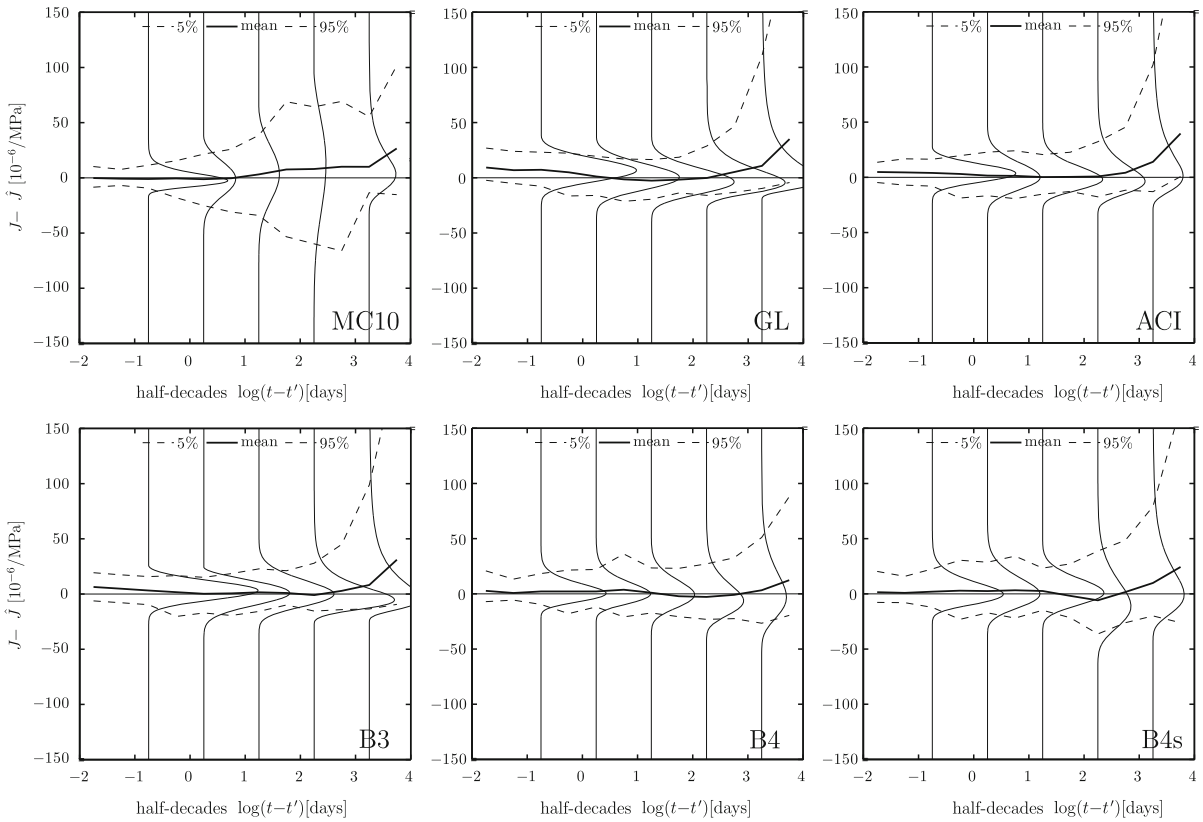

Fig. 11 Development of residuals with $\log(t - t')$ according to prediction model

distribution of scaling factors as discussed in [3] and shown in Fig. 12. The resulting distributions can be approximated by lognormal distributions. These distributions may serve as input for long-term performance predictions and life-time analyses [42–44]. The 5 and 95 % confidence limits based on the fitted distributions of uncertainty factors ψ are: $\psi_{q1} \in [0.6, 1.8]$, $\psi_{q2} = \psi_{q3} \in [0.4, 3.3]$, $\psi_{q4} \in [0.4, 2.7]$, and $\psi_{q5} \in [0.4, 3.1]$.

1.8 Local constitutive law for three-dimensional structural analysis

Analysis of mass structures such as dams or nuclear containments, as well as a realistic analysis of beams, plates, shells and box girders, requires a constitutive law for three-dimensional continuum modeling. The B4 compliance function for basic creep, combined with the principle of superposition and (assumed) constancy of Poisson's ratio, provides a constitutive law in the form of a matrix history integral—a matrix Volterra integral equation with non-convolution kernel. This constitutive law can be converted to a rate-type form; for further details and its application to bridges see, e.g., [45].

Even for basic creep there are limitations to the use of the superposition-based hereditary integrals. One is the temperature rise due to hydration heat, which is neglected here. This is approximately correct only for thin members at constant thermal environment, with moisture sealing but no thermal insulation. Another limitation applies to high-strength concrete, in which the self-desiccation can decrease pore relative humidity to as low as 80 % (compared to about 97 or 98 % in normal concretes).

If the local specific moisture content of concrete and local temperature inside concrete vary, then the present compliance function must first be converted to a rate-type constitutive law based on the Kelvin chain, and then the viscosities of Kelvin units must be replaced by functions of current water content and temperature. Cracking damage, which is the source of

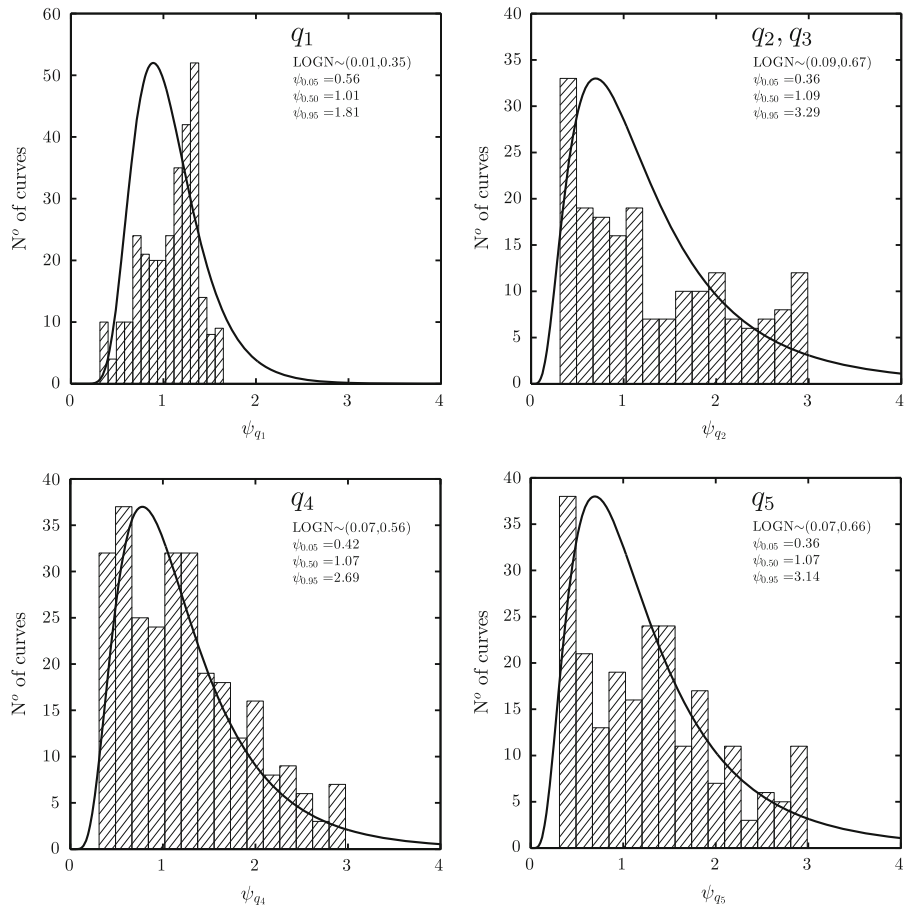

Fig. 12 Development of residuals with $\log(t - t')$ according to prediction model

nonlinearity of concrete creep, must also be modeled. This approach is the same as already approximately demonstrated for Model B3 and its predecessors (see Eq. E1 in [4] or Eq. 1.43 in [7]).

1.9 Concluding comments

1. Overall, model B4 provides the best prediction of creep, as revealed by fitting the collection of over 1500 creep test curves in the NU database and the data on relative multi-decade deflections of 69 bridges. Model B3 comes overall as the second best, with a big gap from B4, and is closely followed by MC10 and GL00.
2. Practically most important is the prediction of creep magnitudes after many decades, and in that regard B4 or B4s is clearly the best, B3 as distant second, and MC10 and GL00 close behind.
3. The ACI92 model, which is almost the same as the original 1971 ACI-209 model [19], is overall the worst. This conclusion is a warning that too much inertia in the codes or standard recommendations harms the engineering practice.
4. It comes as a surprise that model B4s, based solely on concrete strength, performs on average almost as well as the full model B4. Nevertheless, B4s misses the full model's predictive capabilities regarding the influence of composition, aggregate type and admixtures. It is distinctly poorer than B4 in individual fits and predictions (note the scatter plots in the preceding paper, showing how much variation there is even in a narrow band of composition variation). While B4s is a valid design model, B4 should be used for detailed analysis and structural assessment if the composition is known.

5. Even after this extensive optimization effort, there is still too much uncertainty in creep prediction. The main cause of uncertainty is the intrinsic scatter due to small variations in composition.
6. The basic parameters $q_1, \ldots q_5$ of model B4 can be updated in the same way as shown for Model B3, either by Bayesian probabilistic inference [3, 46, 47] or by linear regression in which only scaling factors for the initial value and one common factor for all of the subsequent creep terms are determined [4]. However, based on the experience from the work on model B4, the latter update should be regarded with caution since short-term data used in the update do not provide enough information for the long-term functional form, especially for the drying part of the compliance function. To maintain the correct multi-decade shape of the compliance function and ensure that the term corresponding to the correct mechanisms be assigned to each parameter, only the entire compliance may be scaled. A selective update of parameters associated with a certain time range is possible but may be undertaken only with great care.
7. Future adjustments of model B4 should be made when significant new data become available. The greatest progress could be achieved by new multi-decade data from bridges and other structures, provided that their documentation would suffice for inverse analysis.

Acknowledgments Generous financial support from the U.S. Department of Transportation, provided through Grant 20778 from the Infrastructure Technology Institute of Northwestern University, is gratefully appreciated. So is an additional support under the U.S. National Science Foundation Grants CMMI-1129449 and CMMI-1153494 to Northwestern University. Thanks are also due for additional financial support by the Austrian Federal Ministry of Economy, Family and Youth and the National Foundation for Research, Technology and Development and from the Austrian Science Fund (FWF) in the form of Erwin Schrödinger Scholarship J3619-N13 granted to the first author.

References

1. Hubler MH, Wendner R, Bažant Z P (2014) Comprehensive database for concrete creep and shrinkage: analysis and recommendations for testing and recording. ACI Mater J
2. Bažant ZP, Hubler MH, Wendner R (2014) Model B4 for creep, drying shrinkage and autogenous shrinkage of normal and high-strength concretes with multi-decade applicability. TC-242-MDC multidecade creep and shrinkage of concrete: material model and structural analysis. RILEM Mater Struct
3. Wendner R, Hubler MH, Bažant ZP (2014) Optimization method, choice of form and uncertainty quantification of model B4 using laboratory and multi-decade bridge databases. RILEM Mater Struct
4. Bažant ZP, Baweja S (1995) Creep and shrinkage prediction model for analysis and design of concrete structures: model B3 (RILEM recommendation). Mater Struct 28(6):357–365 Errata, 29, p. 126
5. Bažant ZP, Baweja S (1995) Justification and refinement of Model B3 for concrete creep and shrinkage. 1. Statistics andsensitivity. Mater Struct (RILEM, Paris) 28(7):415–430
6. Bažant ZP, Baweja S (1995) Justification and refinement of Model B3 for concrete creep and shrinkage. 2. Updating and theoretical basis. Mater Struct (RILEM, Paris) 28(8): 488–495
7. Bažant ZP, Baweja S (2000) Creep and shrinkage prediction model for analysis and design of concrete structures: model B3. In: Al-Manaseer A (ed) Adam Neville symposium: creep and shrinkage-structural design effects, ACI SP-194. American Concrete Institute, Farmington Hills, pp 1–83
8. Bažant ZP, Hubler MH, Yu Q (2011) Pervasiveness of excessive segmental bridge deflections: wake-up call for creep. ACI Struct J 108(6):766–774
9. Bažant ZP, Prasannan S (1989) Solidification theory for concrete creep: I. Formulation. J Eng Mech ASCE 115(8): 1691–1703
10. Bažant ZP, Osman E, Thonguthai W (1976) Practical formulation of shrinkage and creep in concrete. Mater Struct (RILEM, Parisi) 9(54):395–406
11. Wittmann F (1971) Kriechverformung des Betons unter statischer und unter dynamischer Belastung. Rheol Acta 10:422–428
12. Çinlar E, Bažant ZP, Osman E (1977) Stochastic process for extrapolating concrete creep. J Eng Mech Div ASCE 103:1069–1088
13. Bažant ZP, Panula L (1978) Practical prediction of time-dependent deformations of concrete. Mater Struct (RILEM, Paris) 11:307–316, 317–328, 415–424
14. Bažant ZP, Carreira D, Walser A (1975) Creep and shrinkage in reactor containment shells. J Struct Div Am Soc Civ Eng 101:2117–2131
15. Bažant ZP, Osman E (1976) Double power law for basic creep of concrete. Mater Struct (RILEM, Parisi) 9(49):3–11
16. Bažant ZP, Osman E (1975) On the choice of creep function for standard recommendations on practical analysis of structures. Cem Concr Res 5:129–138, 631–641; 6:149–153; 7:119–130
17. Committee RILEM, TC-69 (1988) State of the art in mathematical modeling of creep and shrinkage of concrete. Mathematical modeling of creep and shrinkage of concrete. Wiley, New York, pp 57–215
18. Bažant ZP, Hauggaard AB, Baweja S, Ulm F-J (1997) Microprestress-solidification theory for concrete creep. I. Aging and drying effects and II. Algorithm and verification, ASCE. J Eng Mech ASCE 123 (11):1188–1194, 1195–1201
19. Committee ACI 209 (1971) Prediction of concrete creep, shrinkage and temperature effectson concrete structures. In: Designing for effects of concrete creep, shrinkage and

temperature ACI-SP27. American Concrete Institute, Detroit, pp 51–93
20. ACI Committee 209 (1992) Prediction of creep, shrinkage and temperature effects in concrete structures, ACI 209 R-92, American Concrete Institute, Detroit 1992 (minor update of original 1971 version)
21. ACI Committee 209 (2008) Guide for modeling and calculating shrinkage and creep in hardened concrete. ACI Report 209.2R-08, Farmington Hills
22. FIB (1999) Structural concrete: textbook on behaviour, design and performance, updated knowledge of the CEB/FIP model Code 1990. Bulletin No. 2. Fédération internationale du béton (FIB), Lausanne 1:35–52
23. Gardner NJ (2000) Design provisions of shrinkage and creep of concrete. In: Al-Manaseer A (ed) Adam Neville symposium: creep and shrinkage-structural design effect. American Concrete Institute, Farmington Hills, pp 101–104
24. Gardner NJ, Lockman MJ (2001) Design provisions of shrinkage and creep of normal-strength concrete. ACI Mater J 98:159–167
25. FIB (2010) Model code 2010, Fè dè ration internationale de béton, Lausanne
26. Jirásek M, Bažant ZP (2002) Inelastic analysis of structures. Wiley, London
27. Bažant ZP (1972) Prediction of concrete creep effects using age-adjusted effective modulus method. Am Concr Inst J 69:212–217
28. Bažant ZP (1975) Theory of creep and shrinkage in concrete structures: a precis of recent developments. In: Nemat-Nasser S (ed) Mechanics today (American Academy of Mechanical). Pergamon Press, Bažant
29. Trost H (1967) Auswirkungen des sauperpositionsprinzip auf kriech- und relaxations-probleme bei beton und spannbeton. Beton- und Stahlbetonbau 62(230–238):261–269
30. Wang J, Yan P, Yu H (2007) Apparent activiation energy of concrete in early age determined by adiabatic test. J Wuhan Univ Technol 22(3):537–541
31. Poole JL et al (2007) Methods for calculating activation energy Portland Cement. ACI Mater J 104(1):303–311
32. Mindess S, Young JF, Darwin D (2003) Concrete, 2nd edn. Prentice Hall, Englewood Cliffs
33. Rodway LE, Fedirko WM (1989) Superplasticized high volume fly ash concrete. In: Proceedings of the 3rd international conference fly ash, silica fume, slag and natural pozzolans. Trondheim, Norway, pp 98–112
34. Al-Omaishi N, Tadros MK, Seguirant SJ (2009) Elasticity modulus, shrinkage, and creep of high-strength concrete as adopted by ASSHTO. PCI J 54:44–63
35. Persson B (2001) A comparison between mechanical properties of self-compacting concrete and teh corresponding properties of normal concrete. Cem Concr Res 31:193–198
36. Alexander MG (1996) Aggregates and the deformation properties of concrete. ACI Mater J 93(6):569–577
37. Bažant ZP, Yu Q, Li G-H (2012) Excessive long-term deflections of prestressed box girder. Part I: record-span bridge in Palau and other paradigms and Part II: numerical analysis and lessons learned. ASCE J Struct Eng 138(6): 676–686, 687–696
38. Müller HS (1993) Considerations on the development of a database on creep and shrinkage tests. In: Bažant ZP, Carol I (eds) Proceedings of 5th international RILEM symposium on creep and shrinkage of concrete (ConCreep 5), U.P.C., Barcelona, E & FN Spon, London, pp 859–872
39. Vandamme M, Zhang Q, Carrier B, Ulm F-J, Pellenq R, van Damme H, Le Roy R, Zuber B, Gartner E, Termkhajornkit P (2013) Creep properties of cementitious materials from indentation testing: signification, influence of relative humidity, and analogy between C-S-H and clays, keynote presentation, CONCREEP 9, Boston
40. Hubler MH, Wendner R, Bažant ZP (2014) Statistical justification of model B4 for drying and autogenous shrinkage of concrete and comparisons to other models. RILEM Mater Struct
41. Bažant ZP, Yu Q (2013) Relaxation of prestressing steel at varying strain and temperature: viscoplastic constitutive relation. ASCE J Eng Mech 139(7):814–823
42. Strauss A, Hoffmann S, Wendner R, Bergmeister K (2009) Structural assessment and reliability analysis for existing engineering structures, applications for real structures. Struct Infrastruct Eng 5(4):277–286
43. Wendner R, Strauss A, Guggenberger T, Bergmeister K, Teply B (2010) Approach for the assessment of concrete structures subjected to chloride induced deterioration. Beton- und Stahlbetonbau, 105. Heft 12:778–786
44. Strauss A, Wendner R, Bergmeister K, Costa C (2013) Numerically and experimentally based reliability assessment of a concrete bridge subjected to chloride induced deterioration. J Infrastruct Syst 19(2):166–175
45. Yu Q, Bažant ZP, Wendner R (2012) Improved algorithm for efficient and realistic creep: analysis of large creep-sensitive concrete structures. ACI Struct J 109(5):665–676
46. Bažant ZP, Chern J-C (1984) Bayesian statistical prediction of concrete creep and shrinkage. Am Concr Inst J 81:319–330
47. Bažant ZP, Kim Jenn-Keun (1987) Statistical extrapolation of shrinkage data—Part II: Bayesian updating. ACI Mater J 84:83–91
48. Bažant ZP (1975) Theory of creep and shrinkage in concrete structures: a précis of recent developments. Mech Today 2:1–93
49. Bažant ZP (1982) Mathematical models of nonlinear behavior and fracture of concrete. In: Schwer LE (ed) Nonlinear numerical analysis of reinforced concrete. American Society of Mechanical Engineers, New York, pp 1–25
50. Bažant ZP, Yu Q, Li Q, Klein G-H, Křístek V (2010) Excessive deflections of record- span prestressed box girder: lessons learned from the collapse of the Koror–Babeldaob bridge in Palau. ACI Concr Int 32(6):44–52
51. Dilger WH, Wang C (2000) Creep and shrinkage of high-performance concrete. In: Adam Nevillle Symposium: creep and shrinkage-structural design effects. ACI international, Farmington Hills
52. Bažant ZP, Xi Y, Baweja S (1993) Improved prediction model for time-dependent deformations of concrete: Part 7—short form of BP-KX model, statistics and extrapolation of short-term data. Mater Struct 26:567–574
53. RILEM Committee TC-69 (1987) Conclusions for structural analysis and formulation of standard design recommendations, Mater Struct (RILEM, Paris) 20: 395–398; reprinted in ACI Mater J 84:578–581